ON PERFECT IMAGE CORRECTION BY UNSHARP MASKING

Leo Levi* and M. Mossel**

**Jerusalem College of Technology, P.O.B. 16031, Jerusalem*
***National Physical Laboratory, Hebrew U. Campus, Jerusalem*

ABSTRACT

Incoherent image enhancement, such as unsharp masking, is more economical than the coherent techniques, but also more limited. Here the limitations on perfect image de-blurring are investigated. Both linear and non-linear processes are treated and extensive results, based on computer simulation, are presented.

1. Introduction

Unsharp masking is, perhaps, the oldest of the sophisticated methods of image enhancement. Its original implementation, 45 years ago [1], involved the combination of a blurred original negative with a positive copy which was intentionally blurred further: the result was a sharper print. This process was, in effect, a partial equalization of the spatial frequency spectrum. Since then, many processes have been devised, operating in widely different ways, but all in a manner analagous to the above. [2] Some of these involve scanning (with a spot which is either constant [3-7] or dynamically controlled [8] [9]). Simultaneous methods have been developed based on the Herschel effect of photography [10] and on the quenching of photophors. [11, 12] With the exception of the scanning technique using a constant spot, all of these are essentially non-linear processes. These we have analyzed elsewhere [2]. They do not lend themselves to analysis in terms of the transfer function (tf); only in the limiting case of vanishing modulation, do they approach linearity. [2]

Because of this limit, however, and also because of the significance of the constant-spot scanning techniques, the analysis of the linear unsharp masking process is of interest.

2. Linear Unsharp Masking

In the linear version, the primary image spectrum S_1, is the product of the object spectrum, S_o, with the tf, T_o, of the original imaging system. Unsharp masking consists of adding to this spectrum the spectrum, S_m, of the "mask," where the mask is an attenuated and blurred negative version of the primary image. Specifically,

$$S_m = -b\, S_1 T_m \quad ,$$

where T_m is the tf of the blurring process associated with making the mask, and b is the attenuation factor.

It is convenient to express the image signal (s) in terms of

its mean value $\bar{s}$, and its normalized variation:

$$\tilde{s} = s/\bar{s} - 1 .$$

The spectrum of the primary image may then be written;

$$S_1 = \bar{s}_1(\delta + \tilde{S}_1) = \bar{s}_1 (\delta + S_o T_o).$$

where δ stands for $\delta(\nu)$ and represents the Dirac delta function.

We may now write the spectrum resulting from linear masking:

$$S_2 = S_1 + S_m = \bar{s}_1(\delta + S_o T_o) - b\, \bar{s}_1 (\delta + S_o T_o) T_m \qquad (1)$$

$$= \bar{s}_1(1-b) (\delta + \frac{1-bT_m}{1-b} T_o S_o).$$

Here we have made use of the fact that

$$T_m(0) = 1,$$

so that

$$T_m \delta = \delta.$$

Note that the mean signal value has been attenuated by a factor (1-b), showing that b must be maintained below unity. However, since the same attenuation is applied to the signal variation at the origin, the modulation there has not been affected.

To compensate for the attenuation, the signal must be amplified, after masking, by a factor

$$g = 1/(1-b). \qquad (2)$$

3. Multiplicative Masking

In multiplicative masking, it is not the amplitude, but the modulation of the mask that is attenuated by a factor, b. Also, instead of adding it negatively, the sign of the modulation is reversed.

Consider a sinusoidal object function:

$$s_o = \bar{s}_o(1 + M \cos 2\pi\nu).$$

The primary image will be of the form:

$$s_1 = \bar{s}_1 (1 + MT_o \cos 2\pi\nu x),$$

and the blurred mask function:

$$s_m = \bar{s}_m (1-bMT_m T_o \cos 2\pi\nu x).$$

The resulting image then has the form:

$$s_2 = \bar{s}_1 s_m$$

$$= \bar{s}_1 \bar{s}_m [1 + T_o M(1-bT_m) \cos 2\pi\nu x - bT_m T_o^2 M^2 \cos^2 2\pi\nu x]. \qquad (3)$$

We immediately note two fundamental differences between this and the result (1):

(a) In (3) the modulation at the origin is reduced by a factor (1-b), whereas in (1) it remained unaffected.

(b) A term containing $\cos^2 2\pi\nu x = (1 + \cos 4\pi\nu x)/2$ appears. This represents a signal component of twice the object frequency and therefore implies a distortion of the original signal shape. It can be seen that this distortion approaches zero with M^2 and may be negligible for small values of M.

4. Complete Correction

Complete correction by unsharp masking is theoretically possible- but only with linear (i.e. additive) processing. Referring to (1) it is evident that the requirement for this is:

$$(1-bT_m)\, T_o / (1-b) = 1.$$

This is readily seen to imply

$$T_m = (T_o - 1 + b)/bT_o . \qquad (4)$$

This tf becomes negative at the frequency at which T_o drops to the value of (1-b). In the usual optical system, having a low-pass tf, it then rapidly tends toward negative infinity and this limits the implementation of the ideal T_m.

To obtain a practical blurring function, the function (4) may simply be truncated at some convenient value, or it may be damped, for instance, by multiplying it with a bell-shaped curve.

The following considerations indicate the optimum truncation point. Sharp truncation is equivalent to multiplication with a step function and therefore tends to introduce extended oscillations into the corresponding spread function. These, in turn, make physical implementation difficult. This effect may be minimized by truncating the spectrum at its zero-crossing, that is at the spatial frequency, ν_o, where

$$T_o(\nu_o) = 1-b \qquad (5)$$

[Cf. (4) with T_m=0.]

The damping, to be effective, must be stronger than the divergence of the function (4). It has the advantage of suppressing the inconvenient oscillations, but must be expected to yield a less perfect enhancement.

The classical method for preparing the mask is by defocusing. In terms of our ideal correction spectrum (4), this means that we should pick a degree of defocusing, whose blur spread function approximates, as closely as possible, that of the ideal correction spectrum. Here the variables at our disposal are the amount of defocusing (d) and the relative aperture. Rather than the relative aperture we use another parameter derived from it: the (geometrical) blur diameter

$$a = d/F \qquad (6)$$

where F=L/D is the effective F/number of the imaging system,

D is the diameter of the exit pupil of the imaging system and

L is the distance from this pupil to the image plane.

This should be the primary determinant of the mask performance.

5. Results of Computer Simulation

Image enhancement by linear unsharp masking was tested by simulation on a digital computer. Two objects were used:

a. A unit step function
b. A three-bar pattern with gaps between bars equal to the bar width.

These were blurred by a Gaussian spread function (to simulate atmospheric blurring which approaches a near-Gaussian shape on long exposure [13]):

$$T_o(\nu) = e^{-2\pi\sigma_o^2 \nu^2} \quad . \qquad (7)$$

The blurring was normalized by setting the standard deviation, σ_o, equal to unity. The blurred images were then restituted by means of unsharp masks of three types:

a. The ideal function (4) truncated at its zero:

$$T_m(\nu) = 0, \quad \nu > \nu_o,$$

where ν_o is defined by (5).

b. The function (4) again with T_o as given by (7), damped by multiplication with a Gaussian. The standard deviation of this Gaussian was chosen so that the total area under the resulting curve vanishes, i.e. so that the area element above the ν-axis equals that below the axis. The damped correction function then has the form

$$T_m = \{1-(1-b)e^{2\pi^2\nu^2}\} \; e^{-2\pi^2 c^2 \mu^2}/b \qquad (8)$$

where

$$c^2 = 1/[1-(1-b)^2]$$

is the standard deviation of the damping function.

c. The function resulting when an aberrationless lens is defocused. This has the form: [14]

$$T(\nu_r,\Delta) = \frac{4}{\pi}\int_{\nu_r}^{-1} \sqrt{1-u^2} \cos\,[\,2\pi\nu_r\,\Delta(u-\nu_r)]\,du, \quad \nu_r > 1$$

$$= 0, \qquad \nu_r > 1$$

$$\nu_r = \lambda F \nu$$

and has been evaluated accurately over the range ($0<\Delta<100$) where Δ is the defocusing, measured in units of Rayleigh's $\lambda/4$-tolerance on defocusing.[16]

Hence

$$d_R = 2\lambda F^2$$

$$\Delta = d/d_R = d/2\lambda F^2$$

where d is the amount of defocusing and
F is the effective F/number of the system.

The geometrical blur (6) is then

$$a=d/F = 2\lambda F \Delta.$$

For each type of restitution mask, results were computed for four values of b:

$$b= 0,\ 0.5,\ 0.75,\ 0.9,$$

with the application of the corresponding gain values:

$$g= 1,\ 2,\ 4,\ 10.$$

The curve for b=0 represents the uncorrected primary image.

The results are shown in Figs. 1-6. Fig. 1 shows the results obtained with the "ideal" function (4) truncated at the zero-crossing. Figs. 2-5 depict the results obtained with a severely defocused aberrationless lens (Δ = 100) with geometrical blur diameter varying from 1 - 10. In each of these figures are shown (a) the primary blurred step function image (b=0) and the results obtained with b = 0.5, 0.75, 0.9. Also shown are the results obtained with tri-bar patters of unit bar width (b) and of twice this width (c).

The method is not very sensitive to the amount of defocusing: in Fig. 6 we compare the results obtained with Δ = 10 to these with Δ = 100, both for the case of blur diameter a=4.

Results obtained with the damped "ideal" function (8) were quite similar to those shown in Fig.6. They are included in Table 1 described in the next section.

6. Quality Criteria

To compare and evaluate the results, we must first establish image quality criteria.

Classically, such criteria are based on the integrated squared deviation of the image from the object

$$B = 2\int_{o}^{\infty}[1 - s(x)]^2\, dx.$$

To obtain a criterion which correlates positively with image quality, we define the enhancement criterion Q_1, as the reduction in B, normalized with respect to B_o, the value of B obtained in the primary blurred image:

$$Q_1 = (B_o - B)/B_o. \qquad (12)$$

In terms related to the image parameters more directly accessible to measurement, we note that in the case of the step function, the effect of blurring appears as a decrease in the angle of the transition. This angle is maximum at the origin and we may take its value there as a criterion of image quality. In terms of this criterion, all the proposed mask generating methods can yield substantial image enhancement. However, this is invariably accompanied by a distortion of the image contour - in the form of overshoot adjacent to the transition. In an actual system, such overshoots may mask weak (even strong) object detail near a pronounced

contour. The amount of overshoot should therefore enter the quality criterion negatively. We have chosen as the criterion the slope angle θ at the origin divided by the square of the peak height. [This factor is squared in order to permit it to be relatively insignificant for small values of overshoot (h) and to become duly important for large values]. Specifically, this second criterion is defined:

$$Q_2 = 2\theta/\pi \ (1 + h)^2 \tag{13}$$

where the factor $2/\pi$ is introduced to normalize the quality criterion.

Discussion of Results

In Table 1 we list the integrated squared deviation, the angle at the origin and the overshoot for the cases illustrated in Figs. 1-6 and for the damped "ideal" enhancement method. Together with these are listed the quality criteria Q_1 and Q_2.

It can be seen that in all columns the truncated "ideal" filter yields the best results, the advantage becoming more pronounced with increasing enhancement - at b =0.9, the enhancement criterion is superior by about 50% to that of the best factor obtained with defocusing.

REFERENCES

1. G. Spiegler and K. Juris, "Ein neues Verfahren zur Herstellung ausgeglichener Kopien nach besonders harten Originalaufnahmen, " Phot. Korr.67 4-9 (1931). See also ibid 69, 36-41 (1933)

2. L. Levi, "Unsharp Masking and Related Image Enhancement Techniques," Comp. Graph. Image Proc. 3, 163-177 (1974)

3. P. Dumontet, Machine elaborant des produits de composition en vue de la correction de certain defauts dus a la diffraction," Opt. Acta 3 145-6 (1956)

4. R.V. Shack, "Image processing by an Optical Analog Device," Pattern Recog. 2, 123-6 (1970)

5. L. Swindell, " A Noncoherent Optical Analog Image Processor," Appl. Opt.9 2459-69 (1970)

6. S.W. Levine and H. Mate, "Selected Electronic Techniques for Image Enhancement, " Proc. SPIE Image Enhancement Seminar II (1963)

7. W.F. Schreiber, "Wirephoto Quality Improvement by Unsharp Masking, "Pattern Recog. 2, 117-121 (1970)

8. P. Pargas, " The Principle of Velocity Modulation Dodging," Phot.Sci.Eng.9 219-227 (1965)

9. D.R. Craig, "The Log-Etron: A Fully Automatic Servo-Controlled Scanning Light Source for Printing," Phot. Eng. 5, 219-226 (1954)

10. M. Johnson, "Use of the Herschel Effect in Improving Aerial Photographs," J.Opt.Soc. Am. 41, 248-751 (1951)

11. A.J. Watson, "The Fluoro-Dodge Method for Contrast Control," Photogram. Eng.24, 638-643 (1958)

12. A.B. Clarke, " A Photographic Edge Isolation Technique," Photogram.Eng.28 393-9 (1962)

13. D.L. Fried," Optical Resolution through a Randomly Inhomogeneous Medium for Very Long and Very Short Exposures," J. Opt.Soc. Am.56, 1372-9 (1966)

14. L.Levi and R.H. Austing, "Tables of the Modulation Transfer Function of a Defocused Perfect Lens," Appl. Opt.7, 967-974 (1968)

15. L. Levi, Handbook of Tables of Functions for Applied Optics,CRC, Cleveland (1974)

16. E.g. L.Levi, Applied Optics , Wiley (1968) Sect. 9,4,3.

TABLE 1

Blur Function	b = 0.5					b = 0.75					b = 0.9				
	D	$2\theta/\pi$	h	Q_1	Q_2	D	$2\theta/\pi$	h	Q_1	Q_2	D	$2\theta/\pi$	h	Q_1	Q_2
Uncorrected (b=0)	.11685	.241	0	0		-	-	-	-	-	-	-	-	-	-
Ideal correct. trunc.	.0825	.327	.0625	.294	.290	.0694	.381	.075	.406	.329	.0593	.432	.0807	.493	.370
Ideal correct. damped		.353	.107		.288		.456	.253		.290		.639	.730		.213
$\Delta = 100$, a = 1	.113	.248	0	.0329	.248	.107	.261	0	.084	.261	.089	.298	.0088	.238	.293
a = 2	.104	.265	.0013	.110	.265	.0854	.311	.021	.269	.299	.0773	.429	.1491	.338	.325
a = 4	.0861	.309	.0355	.263	.288	.0939	.425	.184	.196	.303	.671	.638	.7081	-4.74	.217
a = 10	.144	.377	.0212	-.232	.256	.983	.562	.699	-7.41	.195	9.77	.786	2.1878	-82.6	.077
$\Delta = 10$, a = 4		.309	.0392		.286		.424	.191		.299		.637	.7198		.215

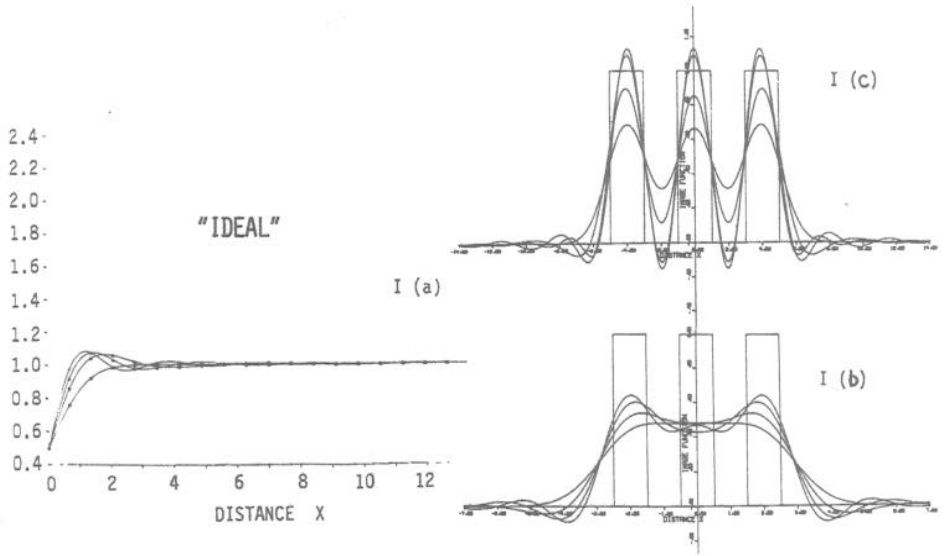

Fig. 1. Results obtained with truncated ideal mask.
a. Unit step function (only upper half is shown)
b. Tri-bar pattern, unity bar width
c. Tri-bar pattern
In each graph, curves shown are for subtraction weights b=0, 0.5, 0.75, 0.9

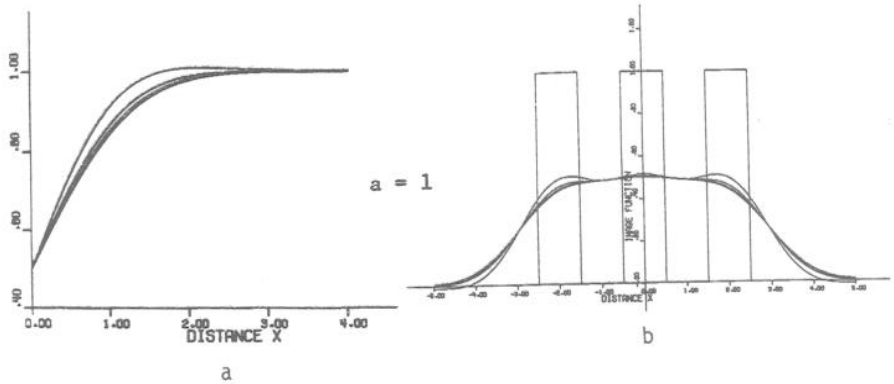

Fig. 2. Results obtained with defocusing - blur diameter: unity
a. Unit step function (only upper half is shown)
b. Tri-bar pattern, unity bar width
c. Tri-bar pattern
In each graph curves shown are for subtraction weights b=0, 0.5, 0.75, 0.9

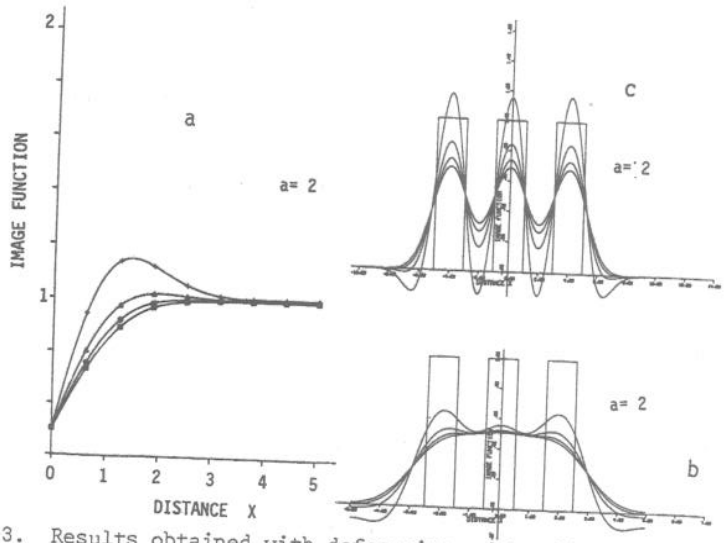

Fig. 3. Results obtained with defocusing - blur diameter: two units
a. Unit step function (only upper half is shown)
b. Tri-bar pattern, unity bar width
c. Tri-bar pattern
In each graph curves shown are for subtraction weights b=0, 0.5, 0.75, 0.9

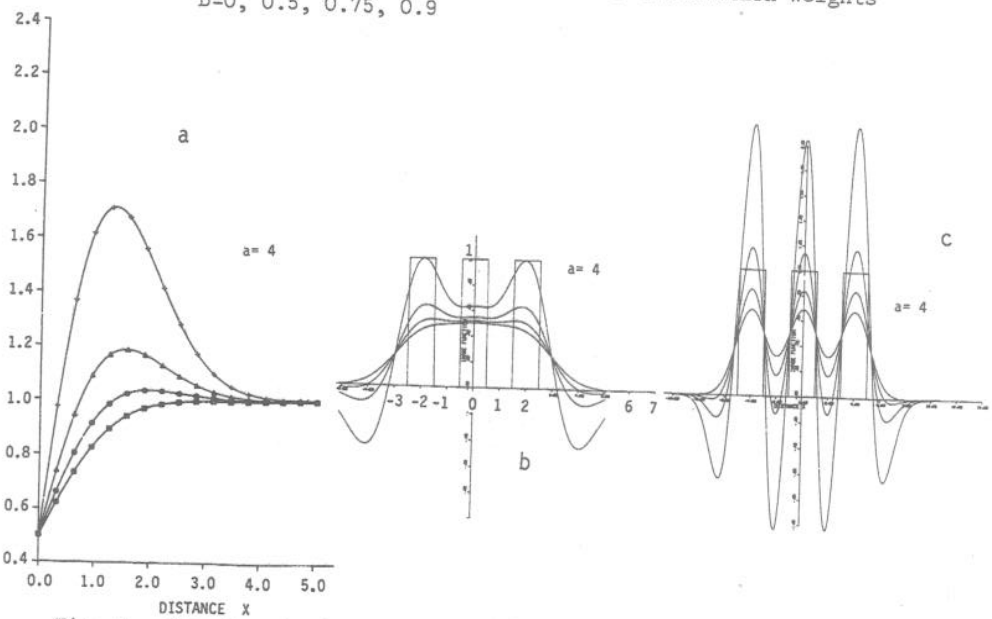

Fig. 4. Results obtained with defocusing - blur diameter four units
a. Unit step function (only upper half is shown)
b. Tri-bar pattern, unity bar width
c. Tri-bar pattern
In each graph curves are for subtraction weights b=0, 0.5, 0.75, 0.9

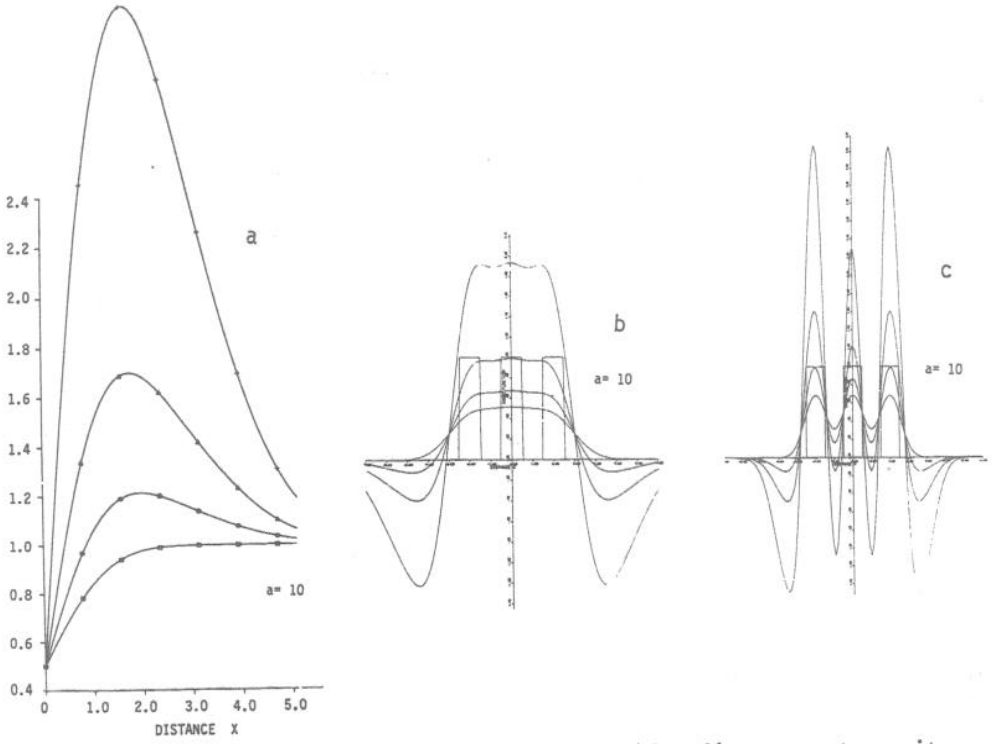

Fig. 5. Results obtained with defocusing - blur diameter: ten units
a. Unit step function (only upper half is shown)
b. Tri-bar pattern, unity bar width
c. Tri-bar pattern
In each graph curves shown are for subtraction weights
b=0, 0.5, 0.75, 0.9

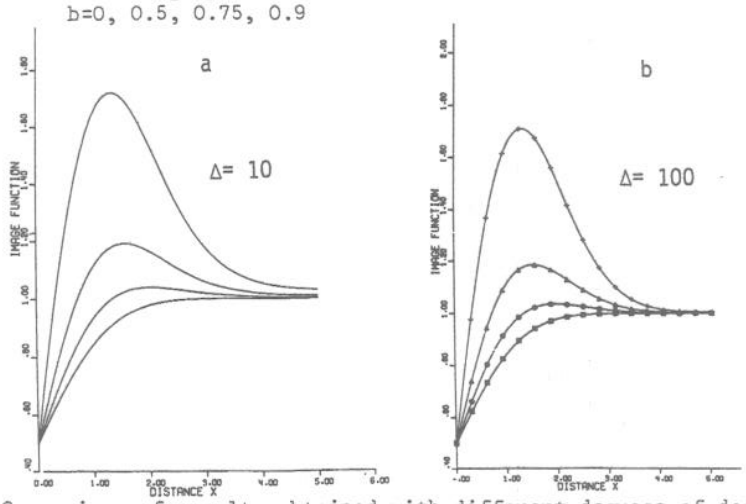

Fig. 6. Comparison of results obtained with different degrees of defocusing
a. Defocusing 10 times Rayleigh's λ/4- criterion tolerance
b. Defocusing 100 times Rayleigh's λ/4- criterion tolerance
In both cases results are for a unit step junction with blur diameters: 4. Curves are shown for subtraction weights
b=0, 0.5, 0.75, 0.9